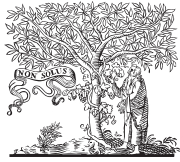


HOSTED BY



ELSEVIER

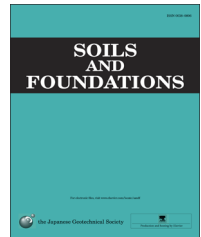


CrossMark

The Japanese Geotechnical Society

Soils and Foundations

www.sciencedirect.com
journal homepage: www.elsevier.com/locate/sandf



Technical Paper

Assessment of methods for construction of an equivalent top loading curve from O-cell test data

Hoyoung Seo*, Rozbeh B. Moghaddam, William D. Lawson

Department of Civil, Environmental, and Construction Engineering, Texas Tech University, Lubbock, TX 79409, USA

Received 2 December 2015; received in revised form 3 June 2016; accepted 28 June 2016
Available online 6 September 2016

Abstract

This paper presents a systematic review of existing methods (original, modified, and load-transfer methods) for constructing an equivalent top loading (ETL) curve using the results of O-cell tests for drilled shaft foundations. The authors performed parametric studies using load-transfer analyses to investigate the effects of the slenderness ratio, foundation stiffness, and the stiffness of the surrounding geomaterials on the elastic shortening of the foundation, which is one of the key components when constructing an ETL curve. Results from the parametric study showed that the foundation compressibility increased with an increasing slenderness ratio, increasing stiffness of the surrounding medium, and decreasing stiffness of the foundation material. It was further shown that when O-cell tests are performed on drilled shafts with very high slenderness ratios or drilled shafts with moderate slenderness ratios, but installed in a very stiff medium, the elastic shortening must be taken into consideration when constructing ETL curves. Full-scale load test data from projects with both the conventional top-down and O-cell load tests performed at the same site were collected and used to assess the validity of the existing ETL methods through three case studies. Analyses of the case studies suggested that the differences among the three existing ETL methods were not significant in terms of ultimate capacity. However, in terms of head settlement, the original ETL method yielded a significantly stiffer load-settlement response than a conventional top-down load test. In contrast, ETL curves constructed by the load-transfer method or the modified method were both practically accurate enough to estimate the head settlement under the service load.

© 2016 The Japanese Geotechnical Society. Production and hosting by Elsevier B.V. This is an open access article under the CC BY-NC-ND license (<http://creativecommons.org/licenses/by-nc-nd/4.0/>).

Keywords: O-cell test; Load test; Equivalent top loading curve; Load-settlement curve; Load-transfer method; Drilled shaft

1. Introduction

Due to the many advantages over the conventional top-down load test, the bidirectional loading test using the Osterberg cell (O-cell) is becoming an increasingly popular way to determine the ultimate capacity of deep foundations. The ultimate capacity of a deep foundation is often defined with reference to a settlement level at the head. A widely used definition of the ultimate resistance of

deep foundations installed in soil is the load that would cause a deep foundation to settle by an amount equal to 10% of its diameter (ISSMFE Subcommittee on Field and Laboratory Testing, 1985; British Standards Institution, 1986; Randolph, 2003; Jardine et al., 2005; Salgado, 2008). In the AASHTO LRFD Bridge Design Specifications (AASHTO, 2012), it is suggested that the ultimate capacity of a drilled shaft be determined as the load corresponding to a 5% relative settlement ($= w_t/B$, where w_t is the head settlement and B is the shaft diameter). In the United States, Davisson's criterion (Davisson, 1972) is widely used to determine the ultimate capacity of driven piles (AASHTO, 2012). Davisson's criterion is performed by first constructing an elastic compression line and then

*Corresponding author.

E-mail address: hoyoung.seo@ttu.edu (H. Seo).

Peer review under responsibility of The Japanese Geotechnical Society.

an offset line parallel to the elastic compression line. Ultimate capacity Q_{ult} corresponds to the load at which the offset line intersects the load-settlement curve. From conventional top-down load tests, the ultimate capacities using 5%, 10%, and Davisson's criterion are easily determined from the measured load-settlement curve.

However, O-cell tests employ a bottom-up loading mechanism instead of the top-down loading mechanism, so the load-settlement curve at the head is not directly measured, but instead must be constructed using the results of O-cell tests. The constructed head load-settlement curve is often referred to as an equivalent top-loading (ETL) curve. The accuracy of ETL curves derived from O-cell data is of critical importance for at least two reasons. First, the ultimate foundation capacities determined with the aforementioned settlement-based criteria will be, at best, as accurate as the constructed ETL curves. To achieve a reliable foundation design, it is very important to obtain the ETL curve under a wide loading range with reasonable accuracy. Second, the determination of the head settlement under the service load has become more important due to the transition of the foundation design framework from the working stress design (WSD) to the load and resistance factor design (LRFD). Recent studies on the performance-based design of drilled shafts are such examples (Roberts et al., 2011; Ng, 2014).

This paper presents a systematic review of the existing methods for constructing ETL curves using the results of O-cell tests. The validity of the ETL methods is critically assessed through a parametric study and field case studies where side-by-side conventional load tests and bidirectional (O-cell) load tests were performed. Load-transfer analyses were used in the parametric study to investigate the influence of the slenderness ratio, concrete stiffness, and soil stiffness on the elastic shortening of the drilled shaft, which is one of the key components when constructing ETL curves. The load test dataset supporting these comparisons is unique in that each test case features both a conventional top-down tested drilled shaft and an O-cell tested drilled shaft in close proximity. Such rare side-by-side load test data facilitate the direct evaluation of the accuracy of the different methods commonly used to construct ETL curves from O-cell data.

2. Review of existing ETL methods

2.1. Original method (Osterberg, 1995)

The results of O-cell tests are typically presented as upward and downward load-displacement curves of the top and bottom plates of the O-cell assembly, respectively. It is expected that the upward load-displacement behavior is governed by the shaft resistance of the test shaft above the O-cell and that the downward behavior is governed by the shaft and base resistances below the O-cell. The original method for constructing ETL curves, suggested by Osterberg (1995) and Schmertmann and Hayes (1997), relies on three main assumptions: (1) the foundation is rigid, (2) the load-displacement behavior of the shaft resistance above the O-cell is independent of the direction of the relative movement between the

foundation and the surrounding soil, and (3) the load-displacement behavior of the foundation below the O-cell is the same as when the shaft is top-loaded.

In the original method, the upward and downward displacement curves are combined by adding the upward and downward loads for common displacements. The upward and downward loads represent the shaft resistance (Q_s) and base resistance (Q_b) above and below the O-cell, respectively, noting that Q_b also includes the shaft resistance of the foundation that is surrounded by the soil below the O-cell. Since the foundation is assumed to be rigid, the common displacements are taken as head settlements (w_t) and the summation of the corresponding loads is taken as the total load (Q_t) at the head.

One of the main drawbacks of the original method is that it ignores the elastic shortening (δ_c) of the foundation material, which could be significantly large when the slenderness ratio of the shaft ($=L/B$, where L and B are the embedment depth below the ground surface and the shaft diameter, respectively) is very large. Another limitation of the original method is that the *direct* summation of the upward and downward displacements is limited to the smaller of the two displacements. To take advantage of larger displacement data, the curve with the smaller displacement must be extrapolated to generate a resulting curve up to the applied load. Hyperbolic curve fitting is typically used for the extrapolation (England, 2009).

2.2. Modified method (Schmertmann, 1998, John H. Schmertmann, personal communication, Nov. 20, 2015)

Unlike the original method, the modified method has not been formally published, although a description of the procedure frequently appears as an Appendix in LOADTEST technical reports. According to Dr. Schmertmann (*personal communication*, November 20, 2015), the modified method was initially suggested by him in 1998 and foundation engineers started using this method as a standard method in August 2000. The modified method is based on the fact that a settlement at the head consists of both the base settlement and the elastic shortening of the foundation material. In O-cell tests, the downward displacement of the bottom plate already includes the base settlement and the elastic shortening of the foundation below the O-cell. Therefore, no additional adjustment is required to account for the elastic shortening of the foundation below the O-cell. However, for the foundation section above the O-cell, the elastic shortening in the equivalent top-down load test mostly exceeds that in O-cell tests (England, 2009).

When loads at the head and at the location of the O-cell are known, elastic shortening $\delta_{c,TLT}$, that would have been obtained from a top-down load test, can be estimated as follows:

$$\delta_{c,TLT} = [C_1 Q_{sO} + (1 - C_1) Q_t] \frac{L_1}{E_p A_p} \quad (1)$$

where Q_{sO} = axial load at the location of the O-cell, Q_t = load at the head, L_1 = length of the foundation between the ground surface and the O-cell, E_p = Young's modulus of the foundation, A_p = cross-sectional area of the foundation, and C_1 = the shape

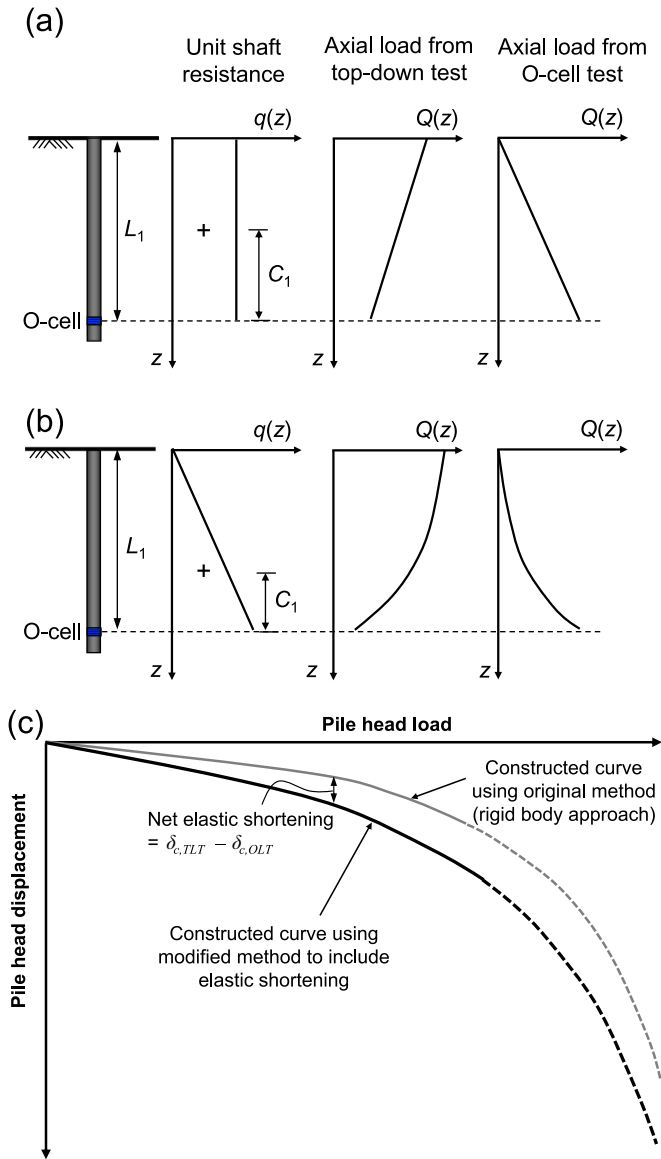


Fig. 1. Distribution of unit shaft resistance and axial load assuming (a) uniform unit shaft resistance ($C_1=0.5$) and (b) linearly increasing unit shaft resistance ($C_1=0.33$); (c) modified ETL curve including elastic shortening.

factor depending on the distribution of unit shaft resistance $q(z)$. Shape factor C_1 is the distance from the location of the O-cell to a centroid of the distribution of unit shaft resistance, as shown in Fig. 1(a) and (b). The values for C_1 can be taken as 0.5 and 0.33 for the uniform and linearly increasing distributions, respectively. Similar values for the shape factors were also used in the analysis to estimate the elastic shortening from conventional top-down tests (Fleming, 1992).

By adding the elastic shortening estimated from Eq. (1) to the ETL curve obtained from the original method, a new ETL curve can be obtained. However, the ETL curve obtained from the original method already includes elastic shortening $\delta_{c,OLT}$, due to the compression load between the O-cell and the foundation head, although the original method assumes the foundation to be a rigid body. Therefore, the elastic shortening $\delta_{c,OLT}$ from the O-cell load tests should be subtracted from the $\delta_{c,TLT}$ estimated from Eq. (1) in order to obtain the net elastic

shortening. Since the load at the head is always zero in the case of O-cell tests (of course, this is not the case with conventional top down load tests), $\delta_{c,OLT}$ can be estimated by replacing Q_t with zero in Eq. (1) as follows:

$$\delta_{c,OLT} = C_1 \frac{Q_{sO}L_1}{E_p A_p} \quad (2)$$

Finally, in the modified method, the net elastic shortening ($=\delta_{c,TLT} - \delta_{c,OLT}$) of the foundation above the O-cell is added to the vertical axis of the ETL curve obtained from the original method. Fig. 1(c) illustrates this.

2.3. Load-transfer method (Coyle and Reese, 1966; Kwon et al., 2005)

The load-transfer method, also known as a $t-z$ analysis, is a technique widely used to study the settlement of a single axially loaded deep foundation, particularly when the soil/rock surrounding the foundation is stratified. This method involves modeling the foundation as a series of elements supported by discrete nonlinear springs which represent the shaft resistances along the shaft ($t-z$ curves) and the base resistance below the foundation base (Q_b-z_b curve). In this method, a base settlement z_b is first specified and the corresponding load at the base is obtained from the Q_b-z_b curve. Then, the load and the settlement at the head are obtained by taking the shaft resistances and the elastic shortening of the foundation segments into account using $t-z$ curves.

Many studies have been performed to investigate the load-transfer behavior of axially loaded deep foundations, and $t-z$ or Q_b-z_b curves were proposed from these studies through theoretical or experimental work (Seed and Reese, 1957; Coyle and Reese, 1966; Coyle and Sulaiman, 1967; Vijayvergiya, 1977; Kraft et al., 1981). The American Petroleum Institute (API, 2011) synthesized results from those studies and proposed $t-z$ and Q_b-z_b curves for axially loaded deep foundations in sandy and clayey soils, which are widely used in practice now. Despite the widespread use of the load-transfer method for the analysis of the settlements of axially loaded deep foundations, very few researchers (Kwon et al., 2005; Lee and Park, 2008; Kim and Mission, 2011) have attempted to apply this method to obtain ETL curves using the results of O-cell load tests. In O-cell load tests, the test shaft is often instrumented with strain gages; and therefore, the $t-z$ curves are readily obtained from the strain gages. The downward load-displacement curve from the O-cell can be directly used as the Q_b-z_b curve.

2.3.1. Practice application of ETL methods

Any O-cell test used to assess the head load-settlement response requires the generation of an ETL curve using one of the aforementioned three methods. A brief summary comparing the main assumptions, advantages, and disadvantages of the three ETL methods is presented in Table 1. Although foundation engineers routinely use the ETL methods described herein, published studies have not quantitatively assessed the frequency of usage of the different methods. According to interviews with LOADTEST engineers (Bob Simpson and Jon

Table 1
Comparison of equivalent top loading (ETL) curve construction methods.

ETL method	Assumptions	Advantages	Disadvantages
Original method (Osterberg, 1995)	<ul style="list-style-type: none"> • The foundation is rigid. • The load-displacement behavior of the shaft resistance above the O-cell is independent of the direction of the relative movement between the foundation and the surrounding soil. • The load-displacement behavior of the foundation below the O-cell is the same as when the shaft is top-loaded. 	<ul style="list-style-type: none"> • The basic concept for creating an equivalent top loading curve is clear. • The procedure is simple and straight forward. • No strain gage data are required. 	<ul style="list-style-type: none"> • The elastic shortening of the foundation material is neglected. • The upward or downward curve with the lesser displacement must be extrapolated to generate a resulting curve up to the applied load. • When test shaft is instrumented, the measured data from the strain gage are not utilized in constructing the ETL curve.
Modified method (Schmertmann, 1998)	<ul style="list-style-type: none"> • The foundation is compressible. • The load-displacement behavior of the shaft resistance above the O-cell is independent of the direction of the relative movement between the foundation and the surrounding soil. • The load-displacement behavior of the foundation below the O-cell is the same as when the shaft is top-loaded. 	<ul style="list-style-type: none"> • The procedure is relatively simple and straight forward. • The elastic shortening of the foundation material is considered. • No strain gage data are required. 	<ul style="list-style-type: none"> • The upward or downward curve with the lesser displacement must be extrapolated to generate a resulting curve up to the applied load. • When the test shaft is instrumented, the measured data from the strain gage are not utilized in constructing the ETL curve.
Load-transfer method (Coyle and Reese, 1966; Kwon et al., 2005)	<ul style="list-style-type: none"> • The foundation is compressible. • The load-displacement behavior of the shaft resistance above the O-cell is independent of the direction of the relative movement between the foundation and the surrounding soil. • The load-displacement behavior of the foundation below the O-cell is the same as when the shaft is top-loaded. 	<ul style="list-style-type: none"> • Maximum utilization of the measured data from O-cells and strain gages can be achieved. • The constructed ETL curve is based on the well-accepted load-transfer analysis method. • The elastic shortening of the foundation material is considered. 	<ul style="list-style-type: none"> • When the unit shaft resistances measured from the strain gages do not reach the limit values, extrapolations are required. • More computational effort is required to generate the ETL curve.

Sinnerich, *personal communication*, March 19, 2015) and with Dr. John H. Schmertmann (*personal communication*, November 20, 2015), LOADTEST considers the original method obsolete in foundation engineering practice. The modified method was the ETL method of choice from August 2000 up through 2010, and the modified method continues to be used today. Since the mid-2000s, the load-transfer method has seen more widespread application (Kwon et al., 2005; Lee and Park, 2008; and Kim and Mission, 2011). The modified method is still the standard, but the load-transfer method is being used as an alternative more and more frequently (Jon Sinnerich, *personal communication*, June 8, 2015).

Given the frequency of usage of the ETL methods, it is reasonable to identify and evaluate the parameters that influence their accuracy. Ultimately, engineers want to know, "How accurate are the different ETL methods?" The remainder of this paper explores the answer to this question through parametric analyses and a side-by-side comparison of top-down load test curves vs. ETL curves generated from O-cell data. Although researchers (Kwon et al., 2005; Lee and Park, 2008; and Kim and Mission, 2011) have attempted to explore the accuracy of ETL curves constructed with the original method and the load-transfer method, none of them has explored the accuracy of the modified method following the procedure described in the earlier section. Furthermore, the studies performed by Kwon et al. (2005) and Lee and Park (2008) were limited to only one load test. To the best of

authors' knowledge, the present study is the first to assess the accuracies of all three methods using at least three load tests.

3. Parametric study

The three key parameters associated with the interpretation of the measured load test data on a drilled shaft include: (1) the slenderness ratio of the drilled shaft, (2) concrete stiffness, and (3) the stiffness of the geomaterials surrounding the drilled shaft. Parametric analyses were performed to explore the influence of each of these factors on the head load-settlement response.

3.1. Effect of slenderness ratio

The load-settlement response of a deep foundation depends on its slenderness ratio, L/B , and can be quite different even in the same soil profile with the same embedment depth. For our parametric study, we consider a 30-m-long drilled shaft, its head flush with the ground surface, with $B=0.3, 0.6, 1.0, 1.5, 2.0,$ and 3.0 m ($L/B=100, 50, 30, 20, 15,$ and 10 , respectively). The maximum unit shaft resistance (t_{max}) and unit base resistance ($q_{b,max}$) were assumed to be 200 kPa and 10,000 kPa, respectively. The $t-z$ and Q_b-z_b curves were generated following the procedures recommended by the

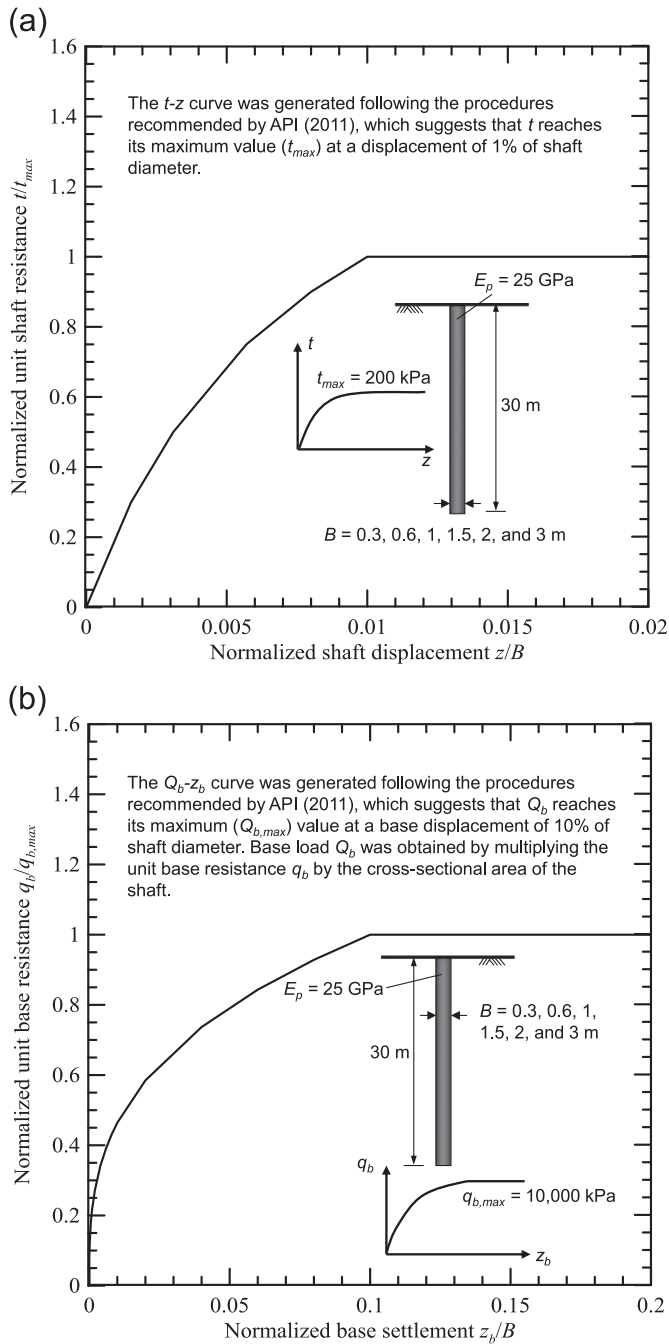


Fig. 2. t - z and q_b - z_b curves used for parametric studies.

American Petroleum Institute (API, 2011), as shown in Fig. 2. Young's modulus E_p of the drilled shaft was assumed to be 25 GPa. Analyses were performed using the commercial software TZPILE Version 2.0.7 (2005), by Ensoft Inc. The drilled shafts in our t - z analysis were subdivided into 50 segments, and calculations were continued until the head settlement reached 5% of the shaft diameter.

To illustrate the effect of the slenderness ratio on the load-settlement response of an axially loaded deep foundation, we present the analysis results for two representative drilled shafts whose diameters are 0.6 and 1.5 m and whose embedment depth is 30 m (therefore, $L/B=50$ and 20, respectively). Figs. 3(a) and

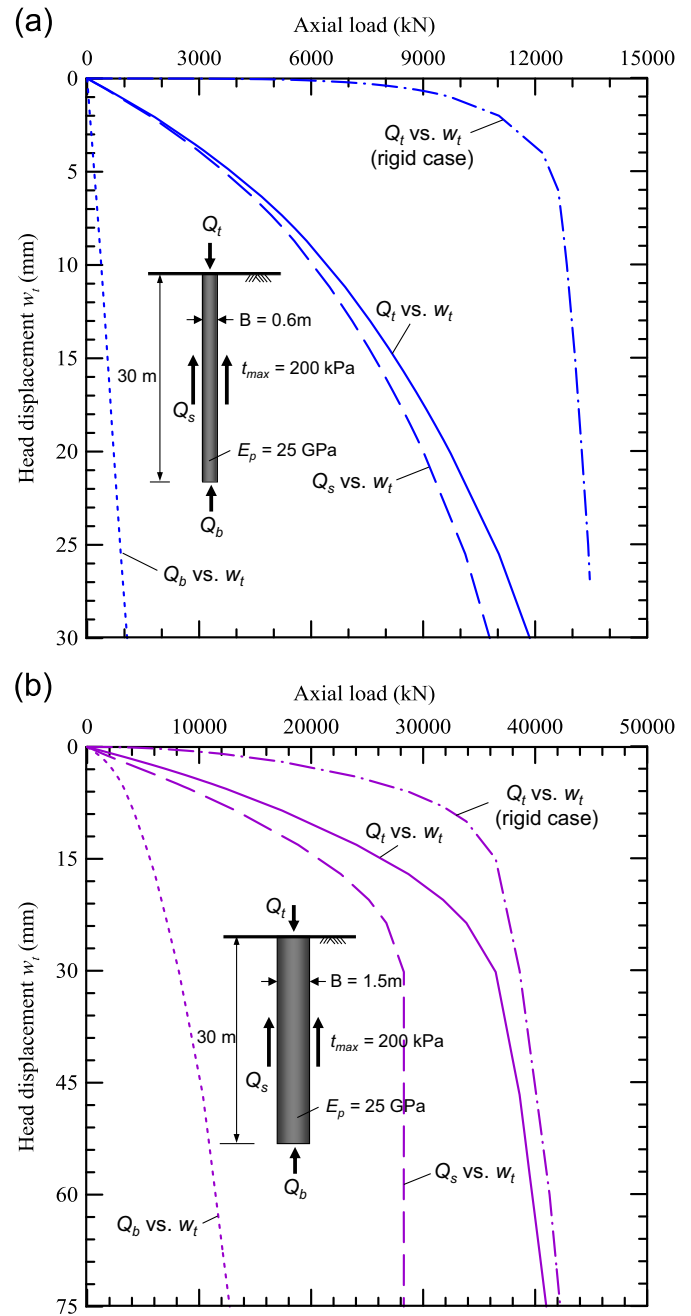


Fig. 3. Loads versus head displacements of 30-m-long drilled shafts with (a) $B=0.6$ m ($L/B=50$) and (b) $B=1.5$ m ($L/B=20$).

(b) show the progression of load Q_t at the head, load Q_s carried by the shaft, and load Q_b transferred to the base versus the head settlement w_t for these drilled shafts. For context, the Q_t versus w_t curves obtained with the assumption that the drilled shaft is rigid are also presented as dashed dot lines in Figs. 3(a) and (b). Fig. 3 (a) clearly shows that, for the drilled shaft with a diameter of 0.6 m, a large difference exists between the load-settlement curves obtained with and without consideration of the elastic shortening of the foundation material. However, the difference decreases for the drilled shaft with a diameter of 1.5 m, as shown in Fig. 3(b). As the slenderness ratios decrease (i.e., the shafts become shorter and stouter), the shafts behave more like rigid bodies, up to the point

where the displacement at the base is almost the same as that at the head. Therefore, for non-slender shafts, the base resistance will be mobilized even in the early loading stages because displacement occurs at the shaft base. On the other hand, shafts with high slenderness ratios are more compressible. As the load at the head increases, the shaft resistance in slender shafts is progressively mobilized along the shaft length and reaches full mobilization at a higher relative settlement level. Fig. 3(a) and (b) suggest that the shaft resistance is fully mobilized at a head settlement of about 30 mm ($w_t/B=2\%$) for the 1.5-m-diameter drilled shaft, whereas the shaft resistance for the 0.6-m-diameter drilled shaft is not fully mobilized until the head settlement reaches about 36 mm or a relative settlement of $w_t/B=6\%$.

Shaft compressibility and the load-transfer behavior over the full range of slenderness ratios are illustrated in Fig. 4. This figure shows the ratio of elastic shortening to head settlement (δ_c/w_t) versus the relative head settlement ($= w_t/B$) up to 5% of the shaft diameter. According to Fig. 4, regardless of the slenderness ratio, the values for δ_c/w_t are approximately equal to 1 for very small head settlements. This means that the head settlement under the very small load stems from elastic shortening only, and is not due to the base settlement. The applied load at the head is then transferred to the base upon further loading; and hence, the shaft base starts settling. Therefore, δ_c/w_t decreases with an increasing w_t/B as more load is transferred to the base. For example, for $B=3$ m ($L/B=10$), δ_c/w_t is initially equal to 1, but quickly drops to a value of about 0.1 (or 10%) at $w_t/B=0.05$. In other words, 90% of the head settlement is due to the settlement at the shaft base when the head settlement reaches 5% of the shaft diameter, which is very close to rigid body behavior. On the other hand, for $B=0.6$ m ($L/B=50$), about 89% of the head settlement results from the elastic shortening of the drilled shaft ($\delta_c/w_t=0.89$) at $w_t/B=0.05$.

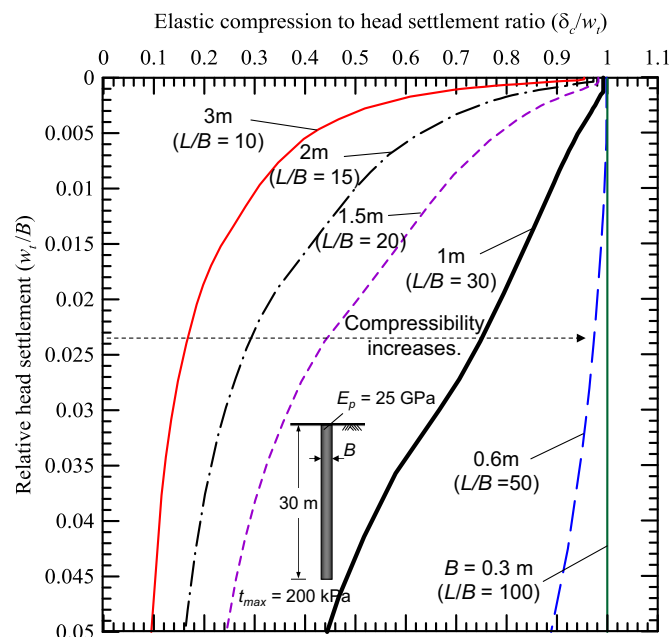


Fig. 4. Elastic compression to head settlement ratio (δ_c/w_t) versus relative head settlement (w_t/B) for various slenderness ratios with t_{max} of 200 kPa.

For a shaft with a very high slenderness ratio ($L/B=100$), δ_c/w_t remains constant at a value of 1 (in other words, the base settlement is zero) for the entire settlement range, meaning that the shaft head settles only due to elastic shortening up to 5% of the shaft diameter. This indicates that for deep foundations with an extremely high slenderness ratio, the base capacity will not be mobilized until the shaft reaches its ultimate limit state. This phenomenon was noticed by earlier researchers as well. Poulos (1982) argued that more than 10% of the head displacement may be required for extremely long foundations ($L/B > 100$) to fully develop their shaft resistance because the foundation becomes very compressible. Furthermore, Randolph (1983) pointed out that foundation slenderness may help explain the apparent decrease, or no increase, in shaft capacity with increasing foundation length reported in the literature, because shaft capacity for a very long foundation may have not reached its maximum value by the time the foundation reaches the settlement at which the load tests are stopped.

Experimental evidence also supports the aforementioned findings. Feng et al. (2015) measured axial strains along two super-long steel pipe piles using the fiber Bragg grating technique during a static load test. Both piles had diameters of 1.5 m and pile lengths of 85.7 m ($L/B=57$) and 78.7 m ($L/B=52$). The two piles were statically loaded up to pile head settlement values of about 1.7% and 2% of the pile diameter, respectively. The measured pile head settlement was reported as being “primarily caused by the compression of the pile body”, and the two test piles “can be treated as pure friction piles because of the zero displacements” at the pile bases. Although the tests were done on driven steel pipe piles and our parametric studies assumed drilled shafts, observations made by Feng et al. (2015) agree well with the results of our analyses. Fig. 4 shows that 98% of the head settlement with $L/B=50$ is due to the elastic shortening of the foundation at $w_t/B=0.02$.

3.1.1. Effect of stiffness of foundation material

For bidirectional testing with O-cells at multiple levels, the stiffness of a drilled shaft can be measured during the load test. However, when an O-cell is installed at a single level, the shaft stiffness cannot be measured, but instead must be estimated using the concrete compressive strength and the amount of reinforcement. In such cases, the estimation of Young's modulus for the test shaft becomes quite important when constructing ETL curves.

According to FHWA Geotechnical Engineering Circular (GEC) No. 10 (Brown et al., 2010), drilled shafts are generally designed with concrete having a specified compressive strength f'_c of 24 to 35 MPa, with a minimum specified compressive strength of 17 MPa. The Young's modulus of concrete E_c with normal weight can be approximated by $E_c=4777(f'_c)^{0.5}$, with both E_c and f'_c in units of MPa (AASHTO, 2012). As mentioned by Brown et al. (2010), the amounts of reinforcement for drilled shafts are typically 1% to 2% and should not exceed 8% of the gross cross-sectional area of the shaft. FHWA GEC No. 10 also recommends that Young's modulus E_{st} for reinforcing steel for drilled shafts be taken as 200 GPa. Assuming that f'_c varies from 17 to 35 MPa and that the reinforcement varies from 1% to 8% of the shaft area, the composite Young's modulus E_p of the drilled

shaft lies in the range of 20 GPa to 40 GPa, with typical values being 25 to 32 GPa.

Fig. 5(a) and (b) show Q_t versus w_t with $E_p=20, 25, 32,$ and 40 GPa for the 0.6-m- and 1.5-m-diameter drilled shafts with the same embedment depth of 30 m ($L/B=50$ and $20,$ respectively). The values for t_{max} and $q_{b,max}$ were assumed to be 200 kPa and 10,000 kPa, respectively. For the drilled shaft with $B = 0.6$ m ($L/B=50$), the settlement values under the same load are quite sensitive to the E_p values (see Fig. 5(a)). This is because the foundation head settles primarily due to elastic shortening for shafts with high slenderness ratios, as seen in Fig. 4. On the other hand, for the drilled shaft with $B = 1.5$ m ($L/B=20$), the settlement responses at the head are similar to each other regardless of the E_p values (see Fig. 5(b)), because the foundation is more rigid; and therefore, the elastic shortening of the shaft contributes less to the head settlement. This analysis indicates that an accurate estimation of Young's modulus becomes quite important for shafts with a high slenderness ratio.

3.1.2. Effect of stiffness of surrounding medium

We now investigate the effect of the stiffness of the surrounding soil or rock on foundation compressibility. Analyses were performed for a drilled shaft with $B=1$ m and $L=30$ m for various values of unit shaft resistance ($t_{max}=50, 100, 150, 200, 300, 500,$ and 2000 kPa). Young's modulus E_p was assumed to be 25 GPa. It may be argued that the elastic shortening of the foundation is affected by the stiffness, not by the strength, of the surrounding soil or rock. In our analysis, however, high t_{max} values also represent high stiffness because API (2011) assumes that t reaches its maximum value at a displacement of 1% of shaft diameter (refer to inset figure, showing $t-z$ curves, in Fig. 6).

Fig. 6 shows δ_c/w_t versus w_t/B for the seven different t_{max} values. Fig. 6 clearly shows that the compressibility of the foundation increases with the increasing stiffness of the surrounding soil or rock – even with the same slenderness ratio. This indicates that foundations with moderately high slenderness ratios may transfer practically no load to the base when the surrounding medium has very high stiffness. Experimental data support this finding. The very same behavior was observed from a static load test performed on a micropile installed in 4.2-m-thick limestone layers (a 2.7-m-thick weathered limestone layer, and a 1.5-m-thick hard limestone layer) overlain by 4-m-thick overburden soils (Seo et al., 2013). The test micropile had a nominal diameter of 0.2 m and an embedment depth of 8.2 m ($L/B=42$ for the entire pile length and 21 for the portion in the rock layer only) and was instrumented with vibrating-wire strain gages. The measured Young's modulus of the test micropile was 90 MPa due to the high reinforcement ratio. A maximum load of 3600 kN was applied at the pile head and the corresponding pile head settlement was 14 mm, 7% of the pile diameter. The average value of the measured unit shaft resistance in the limestone layers was 1455 kPa. Based on the distributions of axial loads measured from the strain gages, researchers reported that about 98% of the maximum applied load (3600 kN) was carried by the shaft. Although the test was

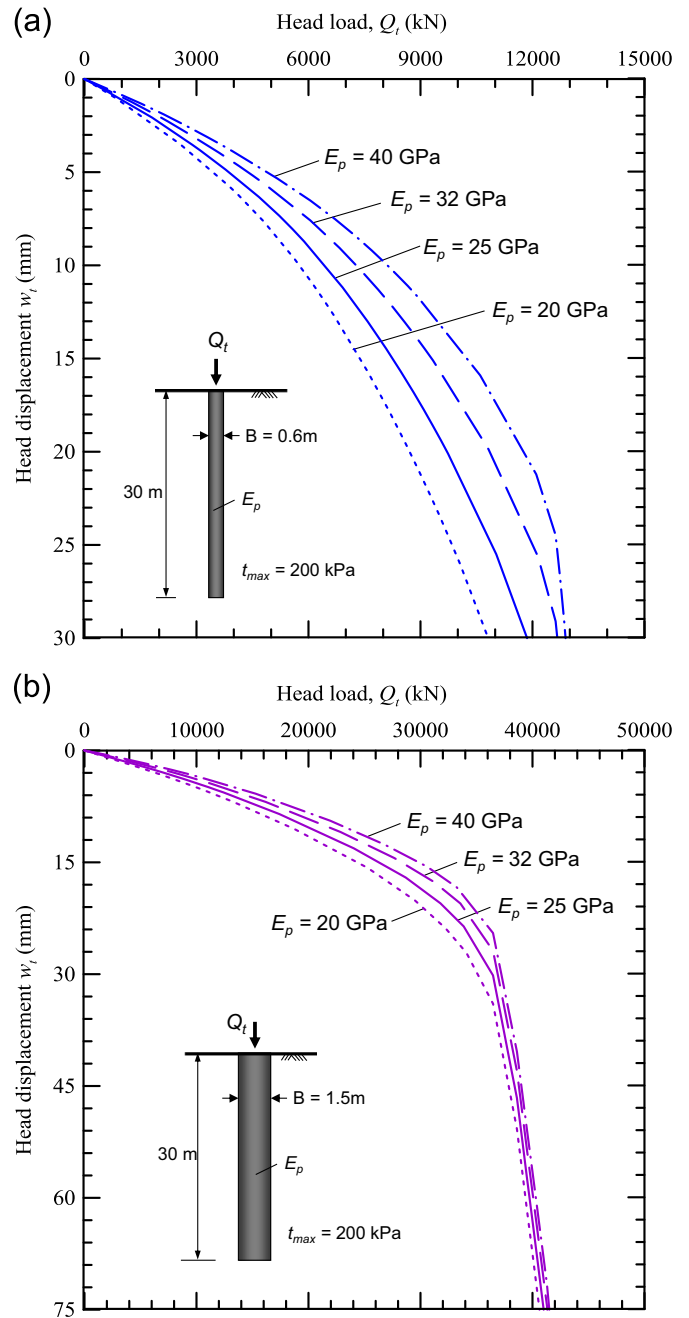


Fig. 5. Head load versus head displacements of 30-m-long drilled shafts for various values of Young's modulus E_p with t_{max} of 200 kPa: (a) $B=0.6$ m ($L/B=50$) and (b) $B=1.5$ ($L/B=20$).

done on a micropile and the values of E_p and L/B reported by researchers differ from those presented in Fig. 6, observations made by Seo et al. (2013) are well in agreement, qualitatively, with the results from our analyses in that most of the applied load is carried by the shaft due to the elastic shortening when the surrounding material is very stiff, such as rock. This much compressibility is not observed in our parametric study for a typical range in t_{max} values for soils (for example, $t_{max}=50$ to 200 kPa) with a foundation slenderness ratio of 30. Fig. 6 indicates that the elastic compression consists of 24 to 44% of total head settlement at $w_t/B=5\%$ when t_{max} lies in the range of 50 to 200 kPa.

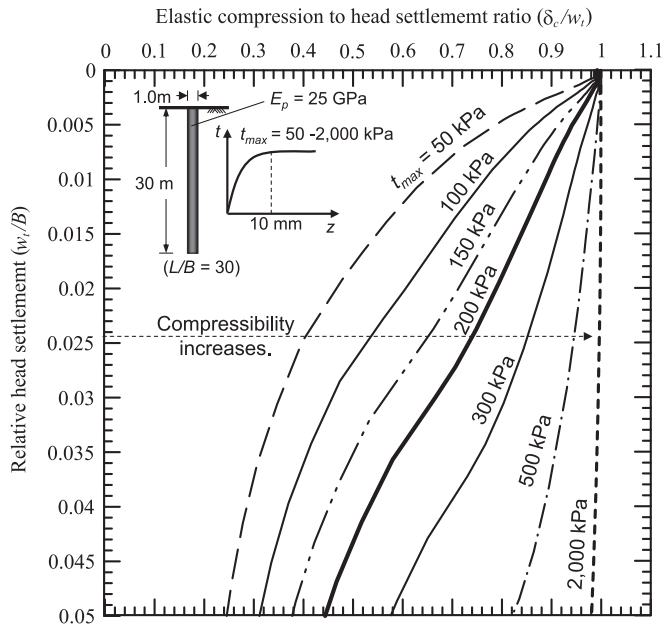


Fig. 6. Elastic compression to head settlement ratio (δ_c/w_i) versus relative head settlement (w_i/B) for t_{max} of 50, 100, 150, 200, 300, 500, and 2000 kPa with $B=1$ m and $L=30$ m.

3.1.3. Parametric study summary

The parametric studies described herein were conducted to investigate the effects of the foundation-soil interaction on the compressibility of drilled shafts using the load-transfer analysis. The results show that the drilled shafts became more compressible as the slenderness ratios increased, the stiffness of geomaterials surrounding the shaft increased, and the stiffness of foundation material decreased. It was further shown that for foundations with an extremely high slenderness ratio, the base capacity may not be mobilized until the foundation reaches its ultimate limit state. These findings are well supported by the experimental observations reported in the literature. On the other hand, for a drilled shaft with a low slenderness ratio, the elastic shortening was negligible and the head settlement was primarily caused by the settlement at the base.

The results from the parametric study clearly suggest that when O-cell tests are performed on foundations with very high slenderness ratios or on foundations with moderate slenderness ratios but installed in a very stiff medium, the elastic shortening must be taken into consideration when constructing ETL curves. Furthermore, it was shown that the estimation of Young's modulus becomes quite important when constructing ETL curves for drilled shafts with very high slenderness ratios or drilled shafts installed in hard rocks.

4. Case studies

To further explore the accuracy of the ETL methods, load test case histories were compiled which contain the data needed to make a direct comparison of head load-settlement curves obtained from actual, full scale, conventional top-down static load tests and O-cell tests performed at the same site in

close proximity. Such load test projects are *exceedingly* rare. In fact, notwithstanding a diligent search and inquiry, the authors were able to identify only three candidate test projects at the time of this study. These include two tests in Singapore in a variety of soils and one test in Korea in highly weathered rock overlain by soil layers. All three tests were performed on drilled shafts with diameters varying from 1.2 m to 1.5 m and embedment depths ranging from 17 m to 37.4 m. The next sections provide detailed information about the site conditions and the results of these three test projects. The O-cell data from these projects were used to construct the ETL curves per the aforementioned methods and these ETL curves were compared with the measured top-down curves.

4.1. Singapore Site A

LOADTEST (2002) and Bored Piling Pte. Ltd. (2002) reported results of an O-cell test and a conventional top-down static load test performed on 1.2-m-diameter drilled shafts at the same site (Fig. 7). The subsurface profile consisted of stiff sandy clay to a depth of 7.8 m with N_{SPT} values from standard penetration testing (SPT) ranging from 10 to 12. Below the stiff sandy clay layer, a dense clayey sand layer was encountered to a depth of 10.4 m with N_{SPT} values ranging from 10 to 66, underlain by a very dense clayey sand layer from below 10.4 m to a depth of about 33 m with N_{SPT} values varying from 66 to greater than 100. The test shafts for the top-down and O-cell load tests were embedded at depths of 17 m and 18.2 m below the ground surface, respectively. The test shaft for the O-cell testing was instrumented with an O-cell at a depth of 11.9 m and with strain gages at various depths below the ground surface. The test shaft for the top-down test was also instrumented with vibrating wire strain gages at various levels.

During the O-cell load testing, the upward shaft resistance reached failure at an upward load of 9340 kN. The reaction system at the shaft head was then engaged to provide additional reaction for the continuation of the test in the downward direction below the O-cell. Fig. 8(a) presents the upward and downward load-displacement curves obtained from the O-cell. The load-transfer curves ($t-z$ curves) for the unit shaft resistance, obtained from the strain gages above the O-cell, are presented in Fig. 8(b).

As the unit shaft resistance values were reported only up to an upward displacement of about 7 mm, which was before the upper shaft resistance reached failure, the $t-z$ curves were extrapolated using a hyperbolic curve-fitting technique in our analysis, as shown in Fig. 8(b). A nonlinear load-displacement behavior of soil has been successfully described using a hyperbolic model (Kondner, 1963; Duncan and Chang, 1970). Similarly, foundation researchers have widely used the hyperbolic model for the soil-shaft interface in the load-settlement analysis (Chin, 1970; Fleming, 1992; Misra and Roberts, 2006; Roberts et al., 2011; Kim and Mission, 2011; Zhang et al., 2014). In Fig. 8(b), the solid lines with symbols represent the measured behavior, while the dashed lines are the extrapolations. Using the load-transfer curves obtained from the strain gages as $t-z$ curves, the load-transfer analyses were performed using the commercial software TZPILE to obtain the ETL curve. For comparison purposes, the upward

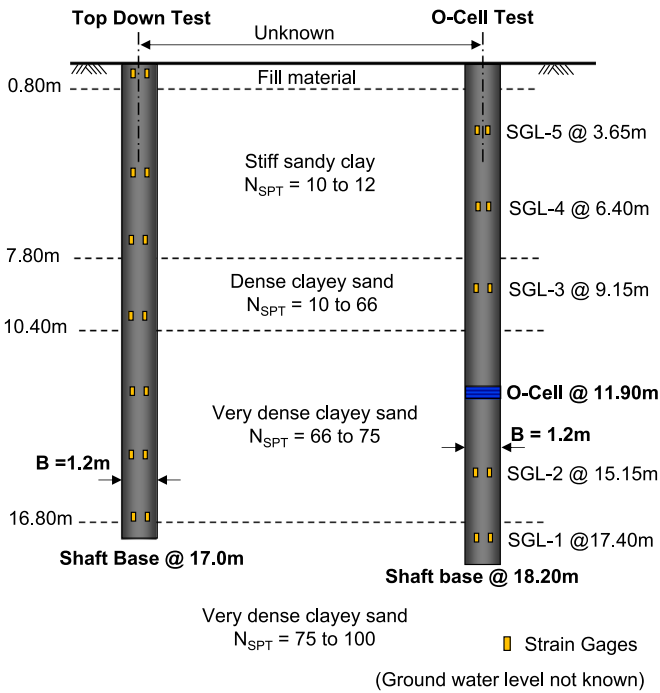


Fig. 7. Soil profile and test shafts at Singapore Site A.

load-displacement curve in Fig. 8(a) was also entered as the $t-z$ curve, representing the entire soil layer above the O-cell as a single layer, and a separate load-transfer analysis was performed. For both cases, the downward load-displacement curve presented in Fig. 8(a) was used as the Q_b-z_b curve. In all our $t-z$ analyses, the test shaft was subdivided into 50 segments. The length of the test shaft was entered as 11.9 m, which is the embedded depth of the O-cell in this case study. The reported value of 37 GPa was used as the Young's modulus (E_p) of the shaft in the analysis.

Fig. 9 shows both the measured top-down load-settlement curve and the ETL curves obtained from the original, modified, and load-transfer methods. Although the ETL curve obtained from the original method shows the stiffest load-settlement response, as expected, all the ETL curves agree reasonably well with the measured head load-displacement curve obtained from the conventional top-down static load test. In particular, both ETL curves constructed with the multiple $t-z$ curves from the strain gages and the single $t-z$ curve constructed with the O-cell show agree very well with the measured top-down curve, except for the range of head load between 15,000 and 20,000 kN. The ETL curve from the modified method also agrees very well with the measured top-down curve. It is interesting to note that the difference between the ETL curves constructed using the original method and the modified method are not significant for this case, and this is attributed to the small amount of elastic shortening due to the low slenderness ratio of the test shaft (L/B is about 15), as was observed in the parametric study.

4.1.1. Singapore Site B

Lee and Park (2008) reported the results of an O-cell test and a conventional top-down static load test performed on 1.2-m-diameter drilled shafts at the Mass Rapid Transit Project site in Singapore (Fig. 10). The soil consisted of silty clay to a

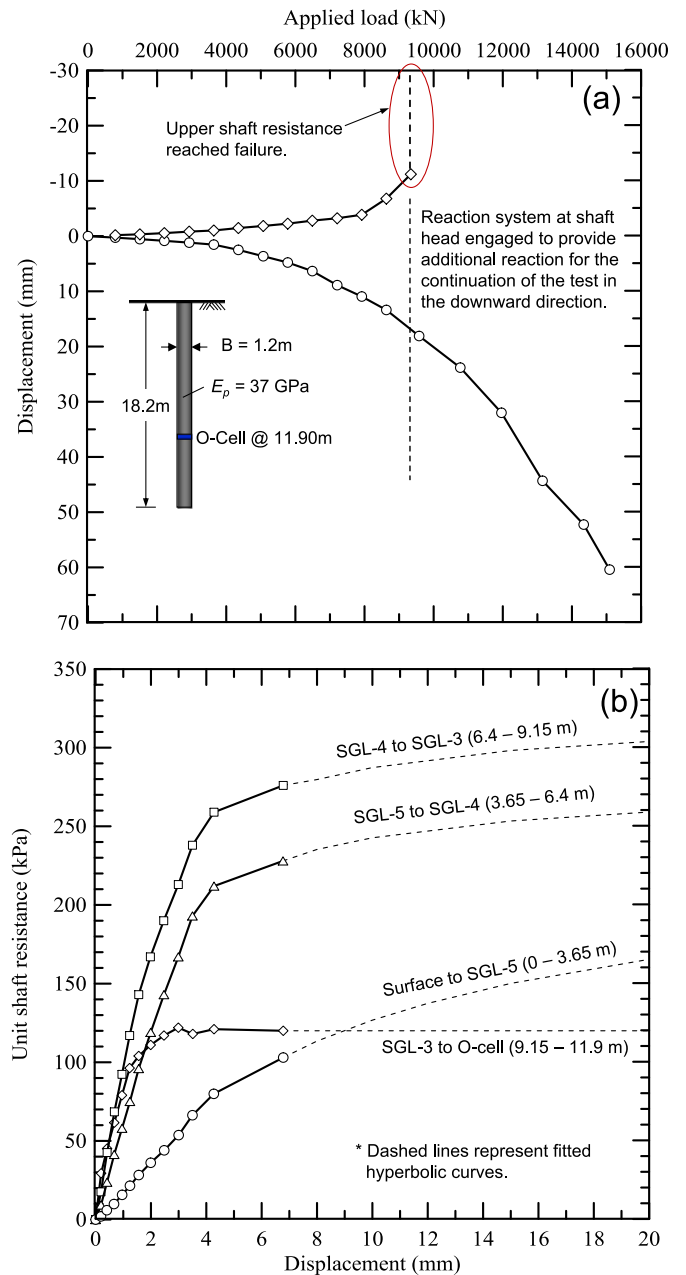


Fig. 8. Results from O-cell testing at Singapore Site A: (a) upward and downward load-displacement curves from O-cell and (b) load-transfer curves from strain gages.

depth of 18.5 m with N_{SPT} values varying from 15 to 31, underlain by stiff clayey silt to a depth of about 37 m with N_{SPT} values ranging from 33 to 81. Below the stiff clayey silt layer, a very stiff silty clay layer was encountered with N_{SPT} values greater than 100. The test shafts for the top-down and the O-cell load tests were embedded at depths of 37 m and 37.4 m below the ground surface, respectively. The test shaft for the O-cell testing was instrumented with two O-cells, namely, the upper O-cell at a depth of 26.9 m and the lower O-cell at a depth of 36.9 m below the ground surface.

As mentioned, two O-cells were employed at different elevations in this case study. With the two levels of O-cells, the test was carried out in three stages. In the first stage, the lower O-cell was pressurized to assess the base and shaft

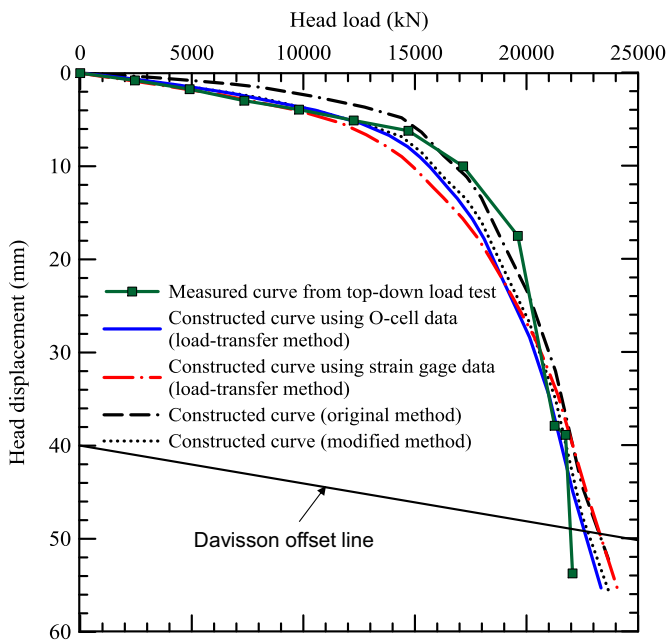


Fig. 9. Comparison of measured and constructed head load-displacement curves for Singapore Site A.

resistances of the test shaft section below and above the lower O-cell, respectively (at this stage, the hydraulic system of upper O-cell was closed off so that the shaft resistance of the test shaft section above the lower O-cell was mobilized as a reaction force). After the completion of Stage 1, the lower O-cell was unloaded in Stage 2. The upper O-cell was then pressurized to assess the shaft resistance of the test shaft section between the two levels of O-cells by utilizing the shaft resistance of the shaft above the upper O-cell as the reaction force (in Stage 2, the hydraulic system of the lower O-cell was left free to drain so that no load was transferred through the O-cell to the base of the test shaft). In the third stage, the hydraulic system of the lower O-cell was closed off, and pressurization of the upper O-cell was continued to assess the shaft resistance of the test shaft section above the upper O-cell. In this paper, only the load-displacement response during Stage 1 is discussed. More details on the testing results from Stages 2 and 3 can be found in the study by Lee and Park (2008). As shown in Fig. 11(a), the mobilized upward resistance was about 9230 kN with upward displacement of about 2.85 mm during loading Stage 1. Similarly, the mobilized downward resistance was about 10,000 kN with downward displacement of about 63 mm.

We constructed ETL curves using the results from Stage 1. The length of the test shaft was entered as 36.9 m, which is the depth of the lower O-cell below the ground surface. Young's modulus E_p of the test shaft was not provided in the paper by Lee and Park (2008); and therefore, it was assumed to vary from 25 to 32 GPa, which is considered to be reasonable for drilled shafts with reinforcements. Kim and Mission (2011) also analyzed the test results presented in Lee and Park (2008) using the ratio of the elastic foundation shortening (called the λ -factor in their article) in the top-down to bottom-up load test and the value of 25 GPa for the E_p in their study.

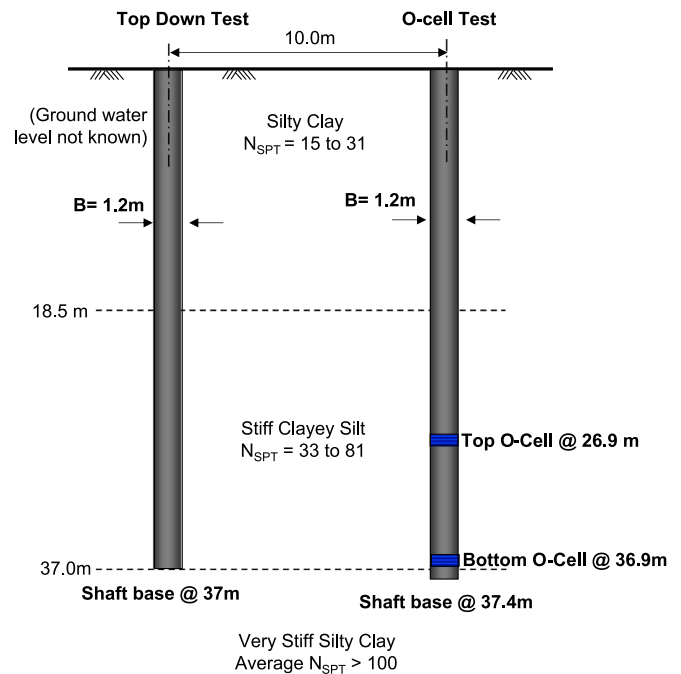


Fig. 10. Soil profile and test shafts at Singapore Site B.

Fig. 11(b) shows a comparison between the ETL curves from various methods and the measured head load-displacement curve from the top-down load test. The ETL curve obtained from Kim and Mission (2011) is also presented for comparison purposes. The ETL curves obtained from the modified and the load-transfer methods agree very well with the measured top-down curve. Furthermore, there was no large difference in the values for E_p in this case study. This case study is of particular interest because the top-down load test was performed until the head settlement reached 116 mm, which is approximately 10% of the shaft diameter, and the ETL curve obtained from the t - z method agrees very well with the measured top-down curve for the entire loading range. It was observed earlier in Fig. 9 that the elastic shortening of the test shaft at Singapore Site A was not significant due to the low slenderness ratio (*i.e.*, $L/B=15$). However, the slenderness ratio L/B of the test shaft at Singapore Site B is about 31, and Fig. 11(b) clearly shows that there is a considerable amount of elastic shortening, which is consistent with the results from our parametric study.

4.1.2. Korea Busan site

Kwon et al. (2005) reported the results of an O-cell test and a conventional top-down static load test performed on 1.5-m-diameter drilled shafts at the same site in Busan, South Korea (Fig. 12). Soil layers consisting of sandy fill, clay, and gravel were encountered to a depth of 28.5 m, underlain by highly weathered rock layers. The gravel and rock layers had N_{SPT} values greater than 50, whereas the N_{SPT} values for the sandy fill and clay layers varied from 5 to 20. The test shafts for the O-cell and top-down load tests, located 9.15 m apart, were embedded at the same depth of 33.5 m below the ground surface. The test shaft for the O-cell testing was instrumented with an O-cell at a depth of 33.5 m, which was also the shaft base, and with strain gages at various depths. The design load

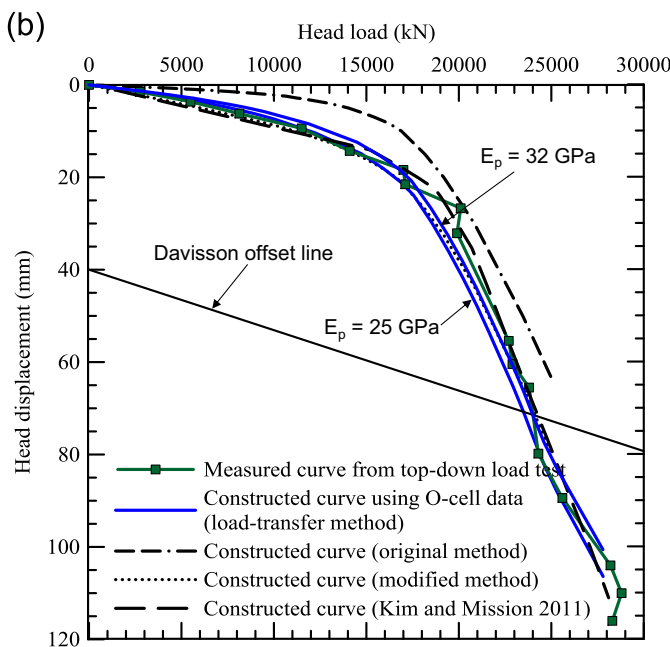
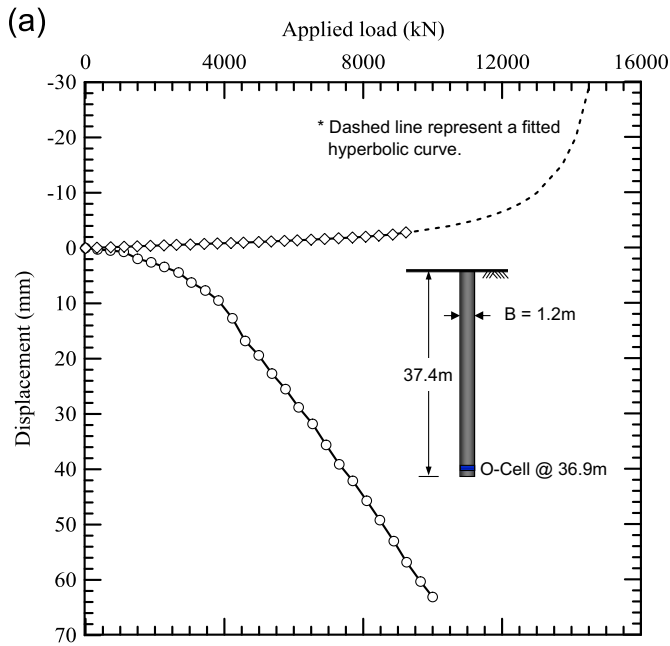


Fig. 11. (a) Upward and download load-displacement curves from O-cell response during Stage 1 and (b) comparison of measured and constructed head load-displacement curves (Singapore Site B).

was 12,000 kN. The test shaft for the top-down load test was also instrumented with strain gages at various levels.

Fig. 13 shows the upward and downward load-displacement curves measured from the O-cell. The load-transfer curves obtained from the soil layers and the rock layers are presented in Fig. 14(a) and (b), respectively. In Figs. 13 and 14, the solid lines with symbols represent the measured behavior and the dashed lines are obtained from extrapolations using hyperbolic curve fitting. It should be noted that in some cases the measured unit shaft resistances showed a softening behavior for which hyperbolic fitting cannot be done. In those cases, the post-peak residual values measured at the maximum

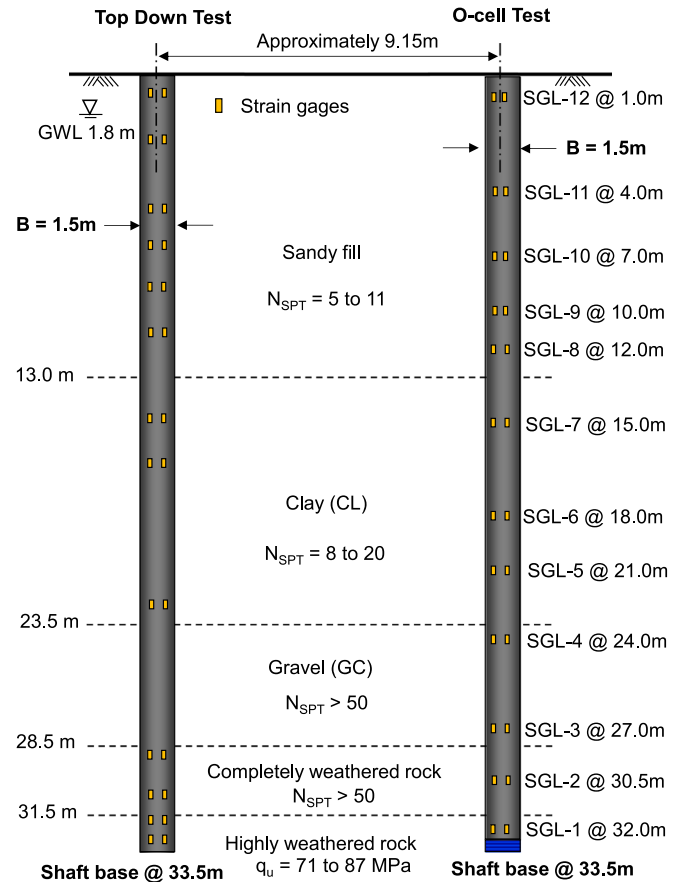


Fig. 12. Soil profile and test shafts at Korea Busan site.

displacements were used as the asymptotic values (*i.e.*, data obtained from depths of 12–18 m and 21–27 m in Fig. 14(a)).

Load-transfer analyses were performed with TZPILE using a) the $t-z$ curves from the strain gages and b) the $t-z$ curve obtained from the O-cell (the upward load-displacement curve in Fig. 13) to construct the ETL curves. For both cases, the downward load-displacement curve was used as the Q_b-z_b curve. As the Young's modulus E_p of the test shaft was not provided in the paper by Kwon et al. (2005), it was assumed to vary from 25 to 32 GPa, as was done previously. The length of the test shaft was entered as 33.5 m in the analysis since the O-cell was installed at the level of shaft base.

Fig. 15 shows a comparison between the ETL curves from various methods and the measured head load-displacement curve from the top-down load test. For comparison purposes, the ETL curve obtained from Kim and Mission (2011) is also presented (Kim and Mission used E_p of 25 GPa in their analysis). The ETL curve obtained with the modified method agrees well with the curves constructed from the load-transfer methods. The slenderness ratio L/B of the test shaft at the Korea Busan Site is about 22 and the values of E_p make little difference in the ETL curves, which is consistent with the results of our parametric study shown in Fig. 5(b). Furthermore, all the ETL curves, except for the one from the original method, agree very well with the measured top-down curve until the head load reaches 20,000 kN. At the design load of 12,000 kN, the head settlement measured from the top-down

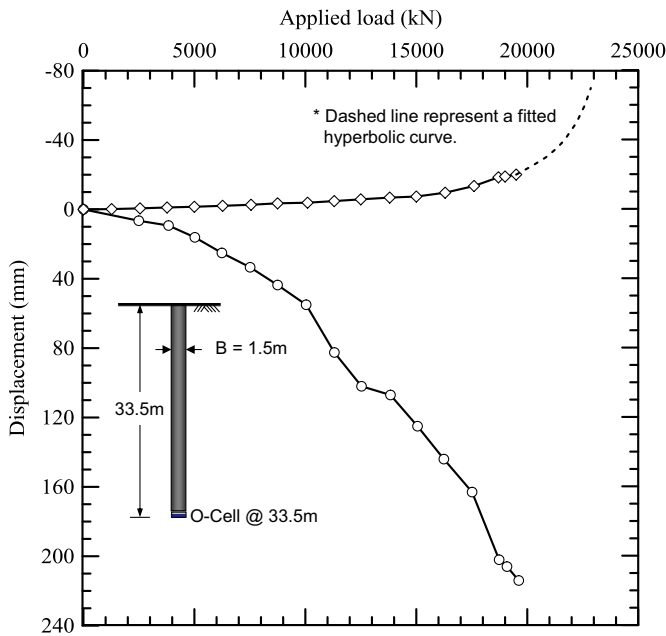


Fig. 13. Upward and download load–displacement curves from O-cell response (Korea Busan site).

load test was about 8 mm. While the head settlements from the ETL curves constructed using the load-transfer analyses and the modified method agreed well with this value, the original method yielded head settlement of about 4 mm, which is one-half of the measured value, illustrating the importance of estimating the elastic shortening. However, the ETL curves obtained from the load-transfer and the modified methods start deviating from the measured curve when the head load becomes greater than 20,000 kN. Kwon et al. (2005) attributed this deviation to “the local dissimilarities of the soil profile at the test [shaft] locations” rather than the shortcomings of the analysis methods. According to Kwon et al. (2005), the maximum shaft resistances at depths between 12.6 and 24.6 m in the clay and gravel layers obtained from the top down load test were “more than two times higher than” those from the O-cell test. Due to the discrepancies in the soil conditions between the top-down test and the O-cell test, Kim and Mission (2011) performed their simulations using the $t-z$ and Q_b-z_b data measured from the top-down test, which showed better agreement with the top-down load-settlement curve, as seen in Fig. 15.

4.2. Case study summary

Collectively, the three case studies provide insight into the accuracy of the ETL methods. Table 2 presents a side-by-side summary of the ultimate capacities and the settlement under the design load as determined from the measured top-down curve and from the constructed ETL curves. Two sources for obtaining $t-z$ curves to generate the load transfer ETL curve are represented, namely, O-cell and strain gages. Interpretations of these data are specific to drilled shafts having diameters of 1.2 m, 1.2 m, and 1.5 m, slenderness ratios of

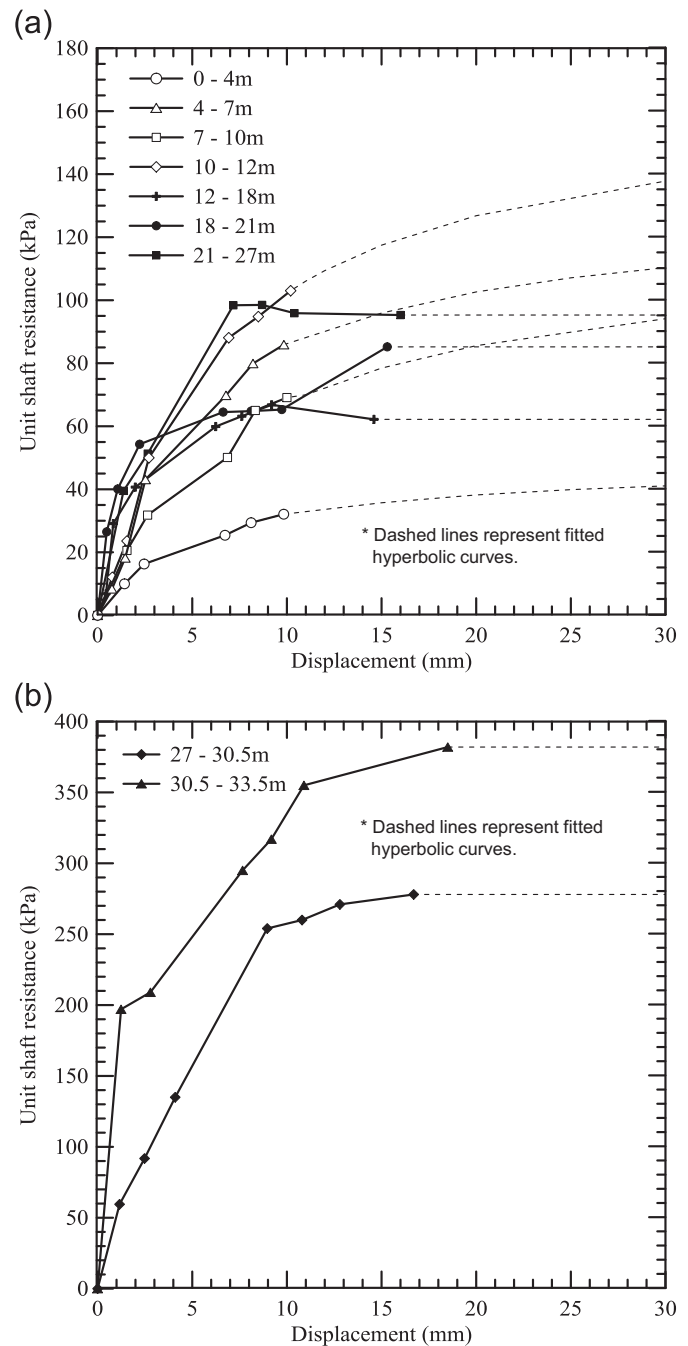


Fig. 14. Load-transfer curves (a) in soil layers and (b) in rock layers (Korea Busan site).

15, 31, and 22, and which are embedded in clayey sand, silty clay, and mixed geomaterials, respectively.

The tabulated values for the ultimate capacity are reasonably consistent for all reported data. The percent difference between the measured capacity determined from the top-down curve versus the ETL curves varies from -2.6% to $+7.4\%$, with an average percent difference of $+2.1\%$. The variance among the ETL capacities is non-significant. The original method provides slightly higher capacity (5.5% to 7.4%), but this is also of no significance for practical applications.

In contrast to the ultimate capacity, significant differences exist between the measured settlement under the design load,

as determined from the top-down curve, versus the ETL curves. Percent differences in settlement for the load transfer and the modified ETL methods vary from -11% to $+11\%$, with an average percent difference of -2% . For the original ETL method, the percent difference in settlement varies from -43% to -67% , with an average percent difference of -55% . The variance among the ETL settlements is significant,

especially for the original method. The estimated settlement under the design load shows that considering the elastic shortening of the foundation when constructing ETL curves (load transfer and modified methods) provides much more accurate load-settlement responses. The original method strongly underdetermines the settlement in these cases.

5. Summary and conclusion

This study has presented a systematic review of the existing methods for constructing ETL curves from O-cell data using a) the original method (rigid body approach), b) the modified method, and c) the load-transfer method. Parametric studies, using the load-transfer method, have been used to investigate the effects of the foundation slenderness ratio, foundation stiffness, and the stiffness of the surrounding medium on the elastic shortening of the foundation. Case studies compiled full-scale load test data from both conventional top-down load tests and O-cell load tests performed at the same site in close proximity. The collected data consisted of three test projects performed on drilled shafts with diameters varying from 1.2 m to 1.5 m and embedment depths ranging from 17 m to 37.4 m (slenderness ratios of the test shafts ranging from 15 to 31). The validity of the different methods used to construct the ETL curves was then assessed.

The results from the parametric study showed that the drilled shafts became, of course, more compressible as the slenderness ratios increased. Less load was transferred to the shaft base and most of the head settlement was due to the elastic shortening of the foundation material when the slenderness ratio of the

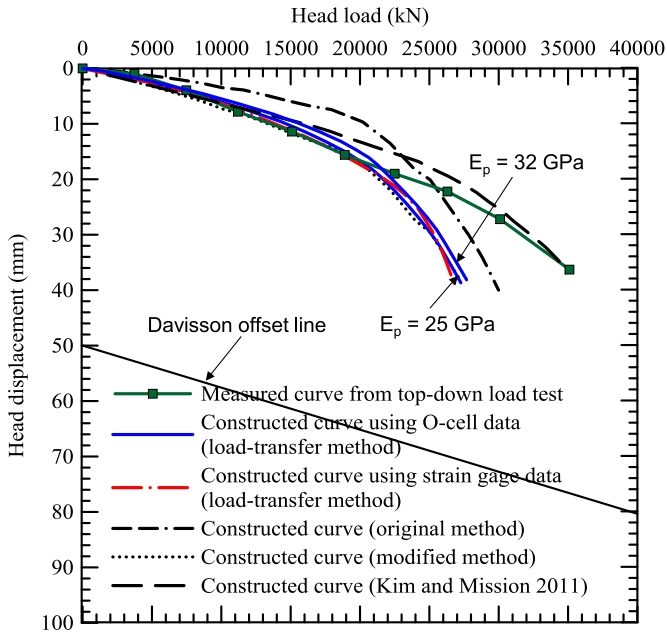


Fig. 15. Comparison of measured and constructed head load-displacement curves for Korea Busan site.

Table 2

Side-by-side comparison of ultimate capacity and head settlement under design load from conventional top-down load test curves (direct measure) and constructed equivalent top loading curves from O-cell test data.

Load test project	Shaft dimensions	Criterion	Top-down	Load transfer method (O-cell)	Load transfer method (Strain gages)	Modified method	Original method
Singapore Site A	$B=1.2\text{ m}$ $L=18.2\text{ m}$ ($L/B=15$)	Davisson	22,000 kN	22,600 kN	23,200 kN	22,650 kN	23,200 kN
		$w_f/B=5\%$ Settlement under Q_d^a	NR ^b 3.92 mm	na 3.63 mm	na 4.04 mm	na 3.62 mm	Na 2.23 mm
Singapore Site B	$B=1.2\text{ m}$ $L=37.4\text{ m}$ ($L/B=31$)	Davisson	24,000 kN	23,500 kN	na ^b	24,000 kN	NR ^b
		$w_f/B=5\%$ Settlement under Q_d^a	22,900 kN 9.23 mm	22,300 kN 9.23 mm	na ^b na ^b	22,900 kN 10.25 mm	24,600 kN 2.88 mm
Korea Busan site	$B=1.5\text{ m}$ $L=33.5\text{ m}$ ($L/B=22$)	Davisson	NR ^b	na ^b	na ^b	na ^b	na ^b
		$w_f/B=5\%$ Settlement under Q_d^a	NR ^b 8.55 mm	na ^b 7.63 mm	na ^b 8.17 mm	na ^b 8.68 mm	na ^b 4.13 mm

^a Q_d =design load (=9807 kN for Singapore A site, 11,300 kN for Singapore B site, and 12,000 kN for Korea Busan site).

^bNR=not reached; na=not applicable.

drilled shaft was very high. On the other hand, for a drilled shaft with a low slenderness ratio, the elastic shortening was negligible and the head settlement was primarily caused by the settlement at the shaft base. The parametric study also showed that the compressibility of a foundation increases with the increasing stiffness of the surrounding medium, even for foundations with the same slenderness ratio. This implies that when O-cell tests are performed on moderately long drilled shafts, but installed in very stiff material such as hard rocks, the elastic shortening must be taken into consideration in the interpretation of the test results. Furthermore, the parametric study indicated that the estimation of Young's modulus of a drilled shaft becomes significant when constructing ETL curves for foundations with very high slenderness ratios.

Analyses of the three case studies suggest that the differences among the three ETL methods are not significant in terms of ultimate capacity. However, the original ETL method, which does not explicitly consider the elastic shortening of the foundation material, yields a significantly stiffer load-settlement response than is measured from a conventional top-down load test in terms of head settlement under the service load. In contrast, the ETL curves constructed with the load-transfer ETL method and the modified ETL method agreed reasonably well with the measured top-down load-settlement response. Furthermore, the source of the t - z curves, whether they were obtained from strain gages or the O-cell, did not introduce any significant discrepancies between the ETL curves. Thus, the case studies indicate that the ETL curves constructed with the load-transfer method or the modified method are both practically accurate enough to estimate the head settlement under the service load.

It should be noted that the available dataset is limited, and load test data from actual, full scale, conventional top-down static load tests and O-cell tests performed at the same site in close proximity are extremely rare. When additional test data become available, other aspects of ETL curve accuracy and reliability, for example, the effect of the degree of the load-transfer curve extrapolation, can be studied.

Acknowledgments

The load test reports for Singapore Site A were provided by LOADTEST USA, Gainesville, Florida. The authors greatly appreciate contributions to this study by Mr. Bob Simpson of LOADTEST and by Mr. Jon Sinnreich of the University of Florida, Gainesville. Moreover, the summary of the history of ETL methods provided by Dr. John H. Schmertmann is highly appreciated.

References

AASHTO, 2012. LRFDP Bridge Design Specifications, 5th ed. American Association of State Highway and Transportation Officials, Washington, D.C.
 API, 2011. API Recommended Practice 2GEO: Geotechnical and Foundation Considerations. American Petroleum Institute.

Bored Piling Pte. Ltd, 2002. Kim Chuan Depot (C821) – Proposed O-cell 1200 mm Area B. Fax Transmission to LOADTEST Asia Pte Ltd Unpublished report.
 British Standards Institution, 1986. Code of practice for foundations. BS8004, London.
 Brown, D.A., Turner, J.P., Castelli, R.J., 2010. Drilled Shafts: Construction Procedures and LRFDP Design Methods. Publication No. FHWA-NHI-10-016/FHWA GEC No. 010, US Department of Transportation/Federal Highway Administration.
 Chin, F.K., 1970. Estimation of the ultimate load of piles from tests not carried to failure. In: Proceedings of 2nd Southeast Asian Conference on Soil Engineering, pp. 81–90.
 Coyle, H.M., Reese, L.C., 1966. Load transfer for axially loaded piles in clay. *J. Soil Mech. Found. Div. ASCE* 92 (SM2), 1–26.
 Coyle, H.M., Sulaiman, I.H., 1967. Skin friction for steel piles in sand. *J. Soil Mech. Found. Div. ASCE*, 93; 261–278.
 Davisson, M.T., 1972. High capacity piles. In: Proceedings of Lecture Series on Innovations in Foundation Construction, ASCE, Illinois Section. Chicago. March 22, pp. 81–112.
 Duncan, J.M., Chang, C.-Y., 1970. Nonlinear analysis of stress and strain in soils. *J. Soil Mech. Found. Div.* 96 (SM5), 1629–1653.
 England, M., 2009. Review of methods of analysis of test results from bi-directional static load tests. In: Proceedings of Deep Foundations on Bored and Auger Piles, Taylor & Francis, pp. 235–239.
 Feng, S., Lu, S., Shi, Z., 2015. Field investigations of two super-long steel pipe piles in offshore areas. *Mar. Georesour. Geotechnol.* <http://dx.doi.org/10.1080/1064119X.2015.1038760> (published online: 11 Sep 2015).
 Fleming, W.G.K., 1992. A new method for single pile settlement prediction and analysis. *Geotechnique* 42 (3), 411–425.
 ISSMFE Subcommittee on Field and Laboratory Testing, 1985. Axial pile loading test - part 1: static loading. *Geotech. Test. J.* 8 (2), 79–90.
 Jardine, R., Chow, F., Overy, R., Standing, J., 2005. ICP Design Methods for Driven Piles in Sands and Clays. Thomas Telford, London.
 Kim, H. -J., Mission, J.L.C., 2011. Improved evaluation of equivalent top-down load-displacement curve from a bottom-up pile load test. *J. Geotech. Geoenviron. Eng.* 137 (6), 568–578.
 Kondner, R.L., 1963. Hyperbolic stress-strain response: cohesive soils. *J. Soil Mech. Found. Div.* 89 (SM1), 115–143.
 Kraft, L.M., Ray, R.P., Kagawa, T., 1981. Theoretical t - z curves. *J. Geotech. Eng. Div.* 107 (11), 1543–1561.
 Kwon, O.S., Choi, Y., Kwon, O., Kim, M.M., 2005. Comparison of the bidirectional load test with the top-down load test. Transportation Research Record No. 1936, Transportation Research Board, pp. 108–116.
 Lee, J.S., Park, Y.H., 2008. Equivalent pile load-head settlement curve using a bi-directional pile load test. *Comput. Geotech.* 35 (2), 124–133.
 LOADTEST, 2002. Data Report: UTP3 – Kim Chuan Depot, Report No. LT-2198-1 (Unpublished report).
 Misra, A., Roberts, L.A., 2006. Probabilistic analysis of drilled shaft service limit state using the “ t - z ” method. *Can. Geotech. J.* 43 (12), 1324–1332.
 Ng, K., 2014. Towards performance based design of drilled shafts. *J. Deep Found. Inst.* 8 (1), 48–55.
 Osterberg, J.O., 1995. FHWA-SA-94-035. The Osterberg Cell for Load Testing Drilled Shaft and Driven Piles. Federal Highway Administration.
 Poulos, H.G., 1982. The influence of shaft length on pile load capacity in clays. *Geotechnique* 32 (2), 145–148.
 Randolph, M.F., 1983. Discussion of 'the influence of shaft length on pile load capacity in clays'. *Geotechnique* 33 (1), 75–76.
 Randolph, M.F., 2003. Science and empiricism in pile foundation design. *Geotechnique* 53 (10), 847–875.
 Roberts, L.A., Fick, D., Misra, A., 2011. Performance-based design of drilled shaft bridge foundations. *J. Bridge Eng.* 16 (6), 749–758.
 Salgado, R., 2008. *The Engineering of Foundation* 1st Ed. McGraw-Hill, New York.
 Schmertmann, J.H., Hayes, J.A., 1997. The osterberg cell and bored pile testing – a symbiosis. In: Proceedings of 3rd International Geotechnical Engineering Conference. Cairo, Egypt, pp. 139–166.

- Seed, H.B., Reese, L.C., 1957. The action of soft clay along friction piles. *ASCE Trans.* 122, 731–754.
- Seo, H., Prezzi, M., Salgado, R., 2013. Instrumented static load test on rock-socketed micropile. *J. Geotech. Geoenviron. Eng.* 139 (12), 2037–2047.
- TZPILE Version 2.0.7, 2005. Computer Software. Ensoft Inc., Austin, Texas.
- Vijayvergiya, V.N., 1977. Load-Movement Characteristics of Piles. In: *Ports 77: 4th Annual Symposium of the Waterway, Port, Coastal and Ocean Division of ASCE, American Society of Civil Engineers*, pp. 269–284.
- Zhang, Q.-Q., Li, S.-C., Liang, F.-Y., Yang, M., Zhang, Q., 2014. Simplified method for settlement prediction of single pile and pile group using a hyperbolic model. *Int. J. Civil. Eng. Trans. B: Geotech. Eng.* 12 (2), 146–159.